JOC The Journal of Organic Chemistry

Note

pubs.acs.org/joc

Design and Construction of *Endo*-Functionalized Multiferrocenyl Hexagons via Coordination-Driven Self-Assembly and Their Electrochemistry

Li-Jun Chen,[†] Quan-Jie Li,[‡] Jiuming He,[§] Hongwei Tan,[‡] Zeper Abliz,[§] and Hai-Bo Yang*[,†]

[†]Shanghai Key Laboratory of Green Chemistry and Chemical Processes, Department of Chemistry, East China Normal University, 3663 North Zhongshan Road, Shanghai 200062, People's Republic of China

[‡]Department of Chemistry, Beijing Normal University, Beijing 100050, People's Republic of China

[§]Institute of Materia Medica, Chinese Academy of Medical Sciences and Peking Union Medical College, Beijing 100050, People's Republic of China

Supporting Information

ABSTRACT: The construction of a new family of *endo*-functionalized multiferrocenyl hexagons with various sizes via coordination-driven self-assembly is described. The structures of these novel metallacycles, containing several ferrocenyl moieties at their interior surface, are characterized by multinuclear NMR (^{31}P and ^{1}H) spectroscopy, cold-spray ionization mass spectrometry (CSI-TOF-MS), elemental analysis, and molecular modeling. Insight into the structural and electrochemical properties of these *endo*-functionalized multiferrocenyl hexagons was obtained through cyclic voltammetry investigation.

Self-assembly of simple building blocks into finite two-dimensional (2-D) and three-dimensional (3-D) supramolecular structures with well-defined shape and size is a prominent field in contemporary chemistry.[1] Over the past few decades, coordination-driven self-assembly has proven to be a powerful tool in the construction of well-defined polygons and polyhedra with increasing structural complexity based on metal−ligand interactions.[2] The highly efficient formation of coordination bonds offers considerable synthetic advantages such as fewer steps, fast and facile construction of the final products, and inherently self-correcting, defect-free assembly. More importantly, with further introduction of various functional moieties on the tectons, a wealth of functionalized supramolecular architectures can be prepared, some of which have exhibited potential applications in the area of molecular recognition and encapsulation, electro- and photochemistry, and catalysis.[3−9] For instance, we have demonstrated that the introduction of crown ether at the vertex of 120° building blocks enables the preparation of 2-D multicrown ethers metallacycles, which have the ability to bind dibenzylammonium guest(s).[5c−f]

As the rigid molecular precursors present a number of different locations where functional moieties can be attached, there are, in general, three means of incorporating functionalities into supramolecular organometallic assemblies.[7] First, incorporation of a functional moiety into the edge or corner of a building block has resulted in a large number of discrete functionalized 2-D polygons.[5a,b,8] For example, the preparation of crown ether and calixarene derivatized building blocks[8a] allowed for the formation of molecular squares with potential host-gust applications. Second, the functional moieties can be covalently grafted on the exterior surface of an angle-directed building block. By employing this approach, we have prepared a variety of *exo*-functionalized squares, rhomboids, rectangles, triangles, and hexagons decorated with Fréchet-type dendrons,[4] crown ethers,[5] and ferrocene units,[6] respectively. Lastly, by covalently attaching a functional moiety to the "inside" of a directional building block with a turning angle less than 180°, a series of *endo*-functionalized supramolecular architectures can be prepared. For instance, Fujita and co-workers have prepared a variety of 3-D *endo*-functionalized $M_{12}L_{24}$ cuboctahedra, which were interiorly decorated with oligo(ethylene oxide) chains, azobenzene units, perfluoroalkyl chains, and polymerizable methyl methacrylate units, respectively.[9] However, compared to many reports about the construction of two-dimensional metallacycles via *exo*-functionalized strategy, the synthesis of *endo*-functionalized discrete polygons is relatively very few. To date, there is only one example of *endo*-functionalization in 2-D metallacyclic complexes to the best of our knowledge.[10]

Ferrocene, as a stable and readily oxidizable organometallic complex, has been widely utilized in multifunctional systems, which have exhibited potential applications in photochemical sensors and information storage.[11] Most multifunctional ferrocenyl compounds have been prepared as, or incorporated

Received: October 11, 2011
Published: December 22, 2011

   dx.doi.org/10.1021/jo201979d | *J. Org. Chem.* 2012, 77, 1148−1153

into, polymers or dendrimers. Typically synthesized using traditional covalent strategies, multifunctional polymers and dendrimers often require considerable synthetic effort and can be plagued by low yields and largely amorphous final structures. By employing ferrocenyl donor and/or acceptor building blocks, coordination-driven self-assembly is able to provide a facile and versatile approach to the construction of multiferrocenyl assemblies, which allows for the precise control over the metallacycle shape, size, and the distribution of ferrocene moieties.[6]

However, compared to many reports on the construction of multiferrocenyl polygongs or polyhedra via *exo-functionalization* strategy, there are rare reports about the synthesis of *endo*-functionalized ferrocenyl supramolecular 2-D polygons. Encouraged by the power and versatility of coordination-driven self-assembly, we envisioned that the construction of *endo*-functionalized ferrocenyl metallacycles with well-designed and controlled cavities would be realized by the proper choice of subunits with predefined angles and symmetry. It is noted that this strategy allows for precise control over the shape and size of the resulting metallacycles as well as the distribution and total number of incorporated ferrocene moieties. The possibility to fine-tuning the size and shape of the final functionalized metallacycles as well as the distribution of electroactive ferrocenes by coordination-driven self-assembly could provide a greater understanding of the influence to electrochemistry caused by structural factors. Moreover, an environmental influence on electrochemistry may occur when ferrocene groups are incorporated into the interior surface of self-assembled supramolecules.[3c,d] Thus, this strategy would likely give rise to the design and synthesis of novel supramolecular species with inspired functionality arising from their unique interior cavities. Herein we report the synthesis and electrochemistry of a new family of multiferrocenyl supramolecular hexagons through *endo*-functionalized approach via coordination-driven self-assembly from a 120° *endo*-ferrocenyl donor ligand and the corresponding di-Pt(II) acceptors.

The 120° ferrocenyl donor precursor **1** can be easily synthesized in a few steps from 4-hydroxy-3,5-diiodobenzoic acid as indicated in Scheme 1. The redox-active ferrocene

Scheme 1. Synthesis of 120° *Endo*-Functionalized Donor Ligand 1

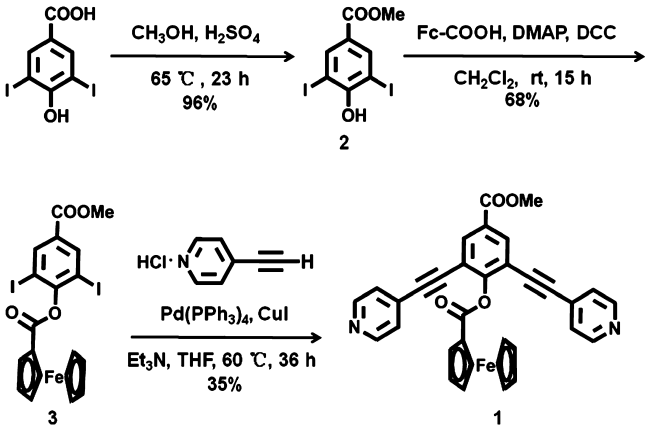

moiety was introduced by a coupling reaction of 2 with ferrocene-1-carboxylic acid. Then Sonogashira coupling of *endo*-functionalized diiodo complex **3** with 4-ethynylpyridine afforded the desired *endo*-functionalized 120° donor ligand **1** in the presence of $Pd(PPh_3)_4$ and CuI as catalysts. Single crystals of ferrocenyl complex **1**, suitable for X-ray diffraction studies, were grown by slow vapor evaporation of a solution of a solvent mixture (ethyl acetate/dichloromethane/petroleum ether 3/2/1) at ambient temperature for 3−4 days. An ORTEP representation of the structure of **1** (Figure S1, Supporting Information) indicates that it is indeed a suitable candidate with the angle between the two pyridine coordination planes being approximately 120°.

The small [3 + 3] molecular hexagon **6** was prepared by mixing the donor ligand **1** with 120° acceptor **4**[2a] in a 1:1 ratio in CD_2Cl_2 (Scheme 2). Multinuclear NMR (^1H and ^{31}P

Scheme 2. Molecular Structures of Donor 1 (Red) and Acceptors 4 and 5 (Blue) and Their Self-Assembly of *Endo*-Functionalized Multiferrocenyl Hexagons 6 and 7

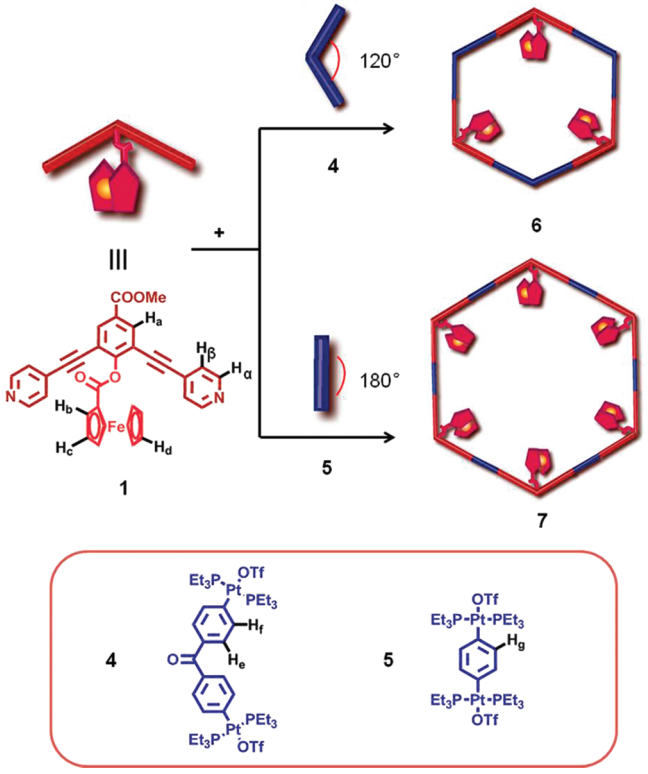

analysis of the reaction mixtures revealed the formation of discrete, highly symmetric species. The ^{31}P $\{^1H\}$ NMR spectrum of **6** (Figure S2A, Supporting Information) displayed a sharp singlet (ca. 13.25 ppm) shifted upfield from the starting platinum acceptor **4** by approximately 6.4 ppm. This change, as well as the decrease in coupling of flanking ^{195}Pt satellites (ca. J = −146 Hz), is consistent with the electron back-donation from the platinum atoms. In the ^1H NMR spectrum of **6**, the α- and β-pyridyl hydrogen signals both experience significant downfield shifts compared with the precursor building block **1** (for α-H, $\Delta\delta$ = 0.10; for β-H, $\Delta\delta$ = 0.40 ppm), which are associated with the loss of electron density upon coordination by the nitrogen lone pair to the platinum metal centers (Figure 1). The investigation of cold-spray ionization mass spectrometry (CSI-TOF-MS) has provided the further support for the existence of *endo*-functionalized hexagon **6**. The CSI-TOF-MS spectrum of **6** exhibited two charge states at m/z = 1281.87 and m/z = 955.65, corresponding to [M − 4OTf]$^{4+}$ and [M −

dx.doi.org/10.1021/jo201979d | J. Org. Chem. 2012, 77, 1148−1153

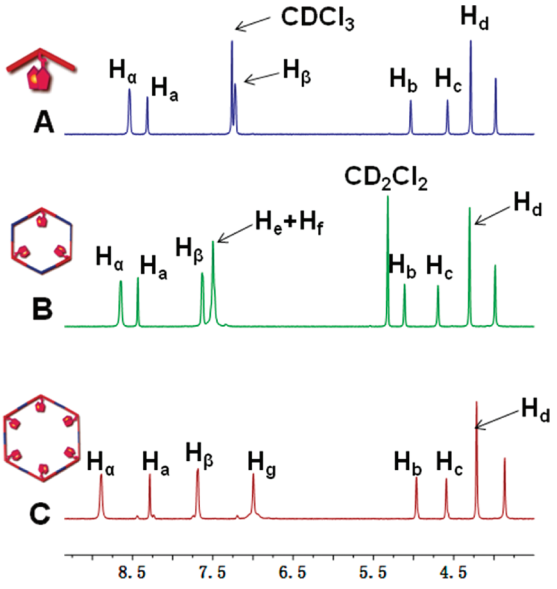

Figure 1. Partial ^{1}H NMR spectra (400 MHz, 298K) of the 120° donor ligand **1** in $CDCl_3$ (A), [3 + 3] hexagon **6** in CD_2Cl_2 (B), and [6 + 6] hexagon **7** in acetone-d_6 (C).

5OTf]$^{5+}$ species, respectively. These peaks were isotopically resolved, and they are in good agreement with their theoretical distributions (Figure S3A, Supporting Information).

When 180° di-Pt(II) acceptor **5**[2b] was employed to react with 120° ferrocenyl donor **1** in a mixed solvent of dichloromethane and acetone (v/v 1/1) in a 1:1 ratio, the large [6 + 6] hexagon **7** with six *endo*-ferrocenyl groups was generated (Scheme 2). The ^{31}P{^{1}H} NMR spectrum of **7** (Figure S2B, Supporting Information) showed a singlet at 14.22 ppm with concomitant ^{195}Pt satellites, upfield shifted by roughly 5.5 ppm compared with the 180° acceptor ligand **5** (δ = 19.68 ppm). Additionally, in the ^{1}H NMR spectrum of **7**, only one set of sharp peaks was found, and the signals displayed characteristic shifts associated with Pt(II)-pyridyl coordination. For example, the significant downfield shifts of the pyridyl α-proton ($\Delta\delta$ = 0.35 ppm) and β-proton ($\Delta\delta$ = 0.45 ppm) were observed, which supported the efficient self-assembly of multiferrocenyl hexagon **7** (Figure 1). In the CSI-TOF-MS spectrum of **7**, the peak at m/z = 2556.25, corresponding to [M − 4OTf]$^{4+}$ species, was observed and its isotopic resolutions are in good agreement with the theoretical distributions (Figure S3B, Supporting Information). Thus the obtained analysis data including the singularity of each ^{31}P NMR signal ensures that only [6 + 6] *endo*-functionalized multiferrocenyl hexagon is formed in the self-assembly.

Unfortunately, all attempts to grow X-ray quality single crystals of the newly designed multiferrocenyl hexagons **6** and **7** have proven to be unsuccessful to date. Therefore, the simulation by PM6 semiempirical molecular orbital method was conducted to gain further insight into the structural characteristics of *endo*-functionalized multiferrocenyl hexagons **6** and **7**. The optimized structure of each multiferrocenyl hexagon featured a very similar, roughly planar hexagonal ring decorated with multiferrocenyl groups at the interior surface (Figure 2). Moreover, the sizes of these novel hexagonal metallacycles were determined as well. For instance, the [3 + 3] hexagon **6** has an internal radius of approximately 2.2 nm, while the [6 + 6] hexagon **7** has a larger internal radius of 3.3 nm. Additionally, it was found that the distance between the nearest two ferrocene units is approximately 1.4 nm for **6** and 1.7 nm for **7**, respectively, which exceeds the distance for the possible interaction between two ferrocene subunits.[6d]

Cyclic voltammetry investigation of ferrocenyl donor **1** as well as multiferrocenyl complexes **6** and **7** was performed in a dichloromethane solution containing 0.2 M n-Bu_4NPF_6 as the supporting electrolyte using a ~7.0 mm^2 glassy carbon disk electrode. In the cyclic voltammogram studies of all complexes the peak current increased systematically with the increase of the scan rates (see the Supporting Information). The cyclic voltammograms corresponding to the one-electron oxidation of ferrocene groups yielded cathodic/anodic peak current ratios of $i_c/i_a \approx 1$. The nearly identical cathodic and anodic peak

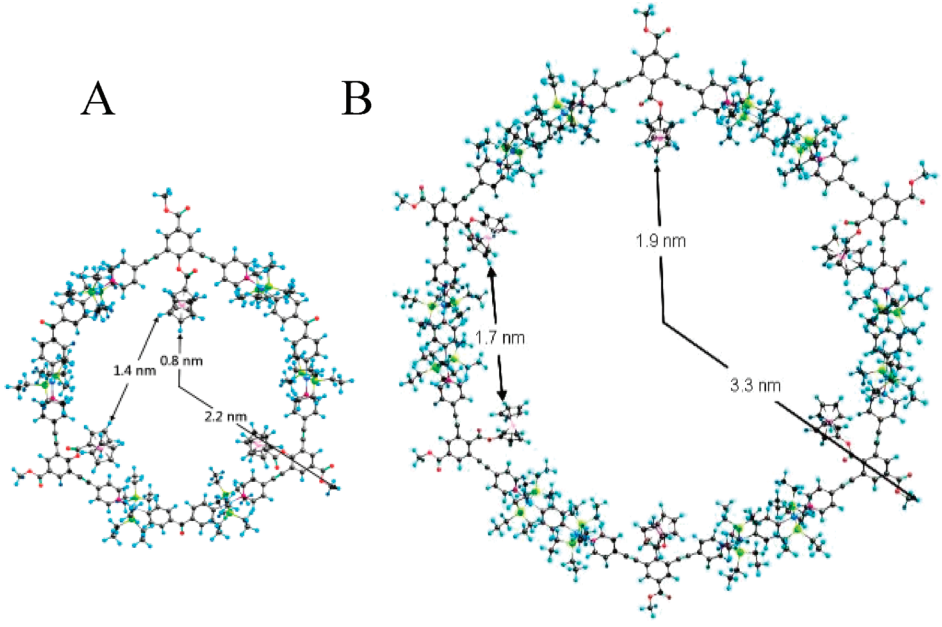

Figure 2. Simulated molecular models of the [3 + 3] hexagon **6** (A) and the [6 + 6] hexagon **7** (B).

dx.doi.org/10.1021/jo201979d | J. Org. Chem. 2012, 77, 1148–1153

currents, as well as nearly scan-rate-independent peak potentials, indicate that the oxidized complexes are chemically stable on the voltammetric time scale and the oxidation of the ferrocene moieties in each assembly is chemically reversible. The potential difference between the anodic and cathodic peak potentials (ΔE_p) was found to be larger than the theoretical value for a reversible redox system (59 mV), which might be partially due to the large ohmic resistance of the CH_2Cl_2 solution.[12] All results demonstrate that the multiple ferrocene groups lack strong intramolecular electronic coupling and react independently, producing a single voltammetric wave, although more than one electron is transferred in the overall reaction. This observation is consistent with the previous reports on electrochemical studies of *exo*-functionalized multiferrocenyl metallacycles.[6] Simulated molecular models further support this result that the well-separated ferrocene building blocks make the Coulombic interaction (through-space electronic coupling) negligible. The half-wave potentials, $E_{1/2}$, measured from the average of voltammetric waves and the potential difference between the anodic and cathodic peak potentials (ΔE_p), are presented in Table S1 in the Supporting Information.

Although the ferrocene-based redox reactions of these complexes are similarly chemically reversible in each case, their electrochemistry is somewhat different. It was found that supramolecular hexagons **6** and **7** featured a 15 and 23 mV positive shifts relative to ligand **1**, respectively (Figures 3). It

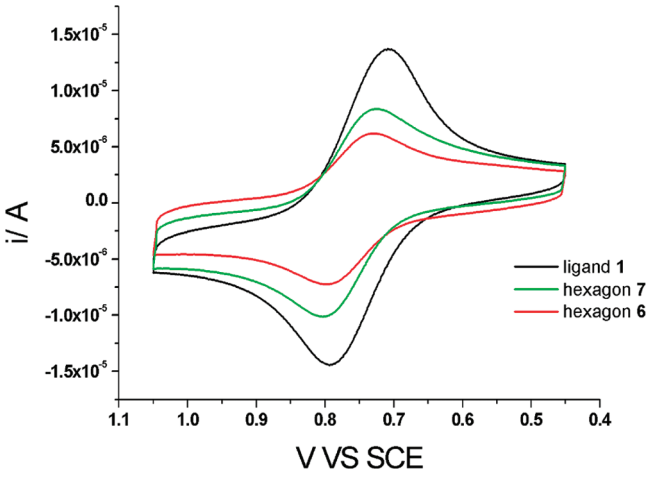

Figure 3. Cyclic voltammetry of 0.2 mM solution of **1** and supramolecular hexagons **6** and **7** (298 K, CH_2Cl_2/0.2 M *n*-Bu_4NPF_6; glassy-carbon electrode with a disk diameter of 3 mm; scan rate at 250 mV/s).

means that it is more difficult to be oxidized for supramolecular hexagons **6** and **7** upon self-assembly, which might be caused by the loss of electron density upon coordination by the nitrogen lone pair to the platinum metal centers. Meanwhile, as shown in Figure 3, the peak current of ligand **1** was larger than that of triferrocenyl hexagon **6** and hexakisferrocenyl hexagon **7**, although two self-assemblies have more electro-active ferrocene sites under the same conditions. This result is obviously different from the previous reports about the electrochemical behavior of *exo*-functionalized multiferrocenyl complexes in literature.[6a−c] To gain further insight into the structural influence, concentration-dependent cyclic voltammetry investigation of compound **1**, **6**, and **7** were carried out (see the Supporting Information). It was found that the current response increased with the increase of ferrocene concentration, yet not with a linear current response. It is obvious that the environmental influence on electrochemistry cannot be negligible when ferrocene groups incorporated into the interior surface of supramolecular metallacycles. In this case, upon self-assembly of *endo*-functionalized multiferrocenyl hexagons, all ferrocenyl units are located in the inner surface of the metallacycles, which makes it difficult to access to the electrode, thus resulting lower magnitude of the current.

In conclusion, we have successfully prepared a new family of *endo*-functionalized multiferrocenyl hexagons by the self-assembly of a new 120° ferrocenyl donor ligand **1** with two different di-Pt(II) acceptors. The synthesis is straightforward and the yield is quantitative, thus eliminating the need of purification. All functionalized metallacycles with several ferrocenyl moieties at their interior surface are characterized with multinuclear NMR (^{31}P and ^{1}H), CSI-TOF-MS, elemental analysis along with molecular modeling. Electrochemical studies revealed that all *endo*-functionalized multiferrocenyl hexagons show reversible one-electron reaction responses. Moreover, a stable and independent reversible redox process, which was somewhat influenced by the supramolecular scaffold, could be observed in the investigation of cyclic voltammetry. These findings provided an enhanced understanding of the influence of structural factors on the electrochemistry of *endo*-functionalized multiferrocenyl metallocycles, which will be helpful in the design and synthesis of novel multiple electro-active supramolecular architectures in the future.

EXPERIMENTAL SECTION

Synthesis of Compound 3. To a solution of ferrocene-1-carboxylic acid (626.4 mg, 2.72 mmol) in 50 mL of anhydrous dichloromethane was added a catalytic amount (10%) of DMAP and 4-hydroxy-3,5-diiodobenzoate (1.0 g, 2.48 mmol). DCC (510.8 mg, 2.48 mmol) was then added to the reaction mixture at 0 °C, followed by stirring for 5 min at 0 °C and 5 h at room temperature. Precipitated urea was filtered, and then the filtrate was evaporated under vacuo. The residue was taken up in 50 mL of CH_2Cl_2, washed twice with 0.5 N HCl and with satd $NaHCO_3$ solution, and then dried over $MgSO_4$. The residue was purified by column chromatography on silica gel (ethyl acetate/petroleum ether 1/5) to give compound **3** as an orange-colored solid. Yield: 1.03 g, 68%. Mp: 219−220 °C. ^{1}H NMR ($CDCl_3$, 400 MHz): δ 3.93 (s, 3H), 4.46 (s, 5H), 4.57 (s, 2H), 5.03 (s, 2H), 8.49 (s, 2H). ^{13}C NMR($CDCl_3$, 100 MHz): δ 52.70, 70.20, 71.03, 72.07, 90.31, 130.52, 140.91, 155.63, 163.63, 168.19. MS (EI): 616 (M^+, 18), 617 [$(M + 1)^+$, 1], 92 (59), 121 (72), 129 (100), 185 (69), 213 (84); HRMS (EI): exact mass calcd for $C_{19}H_{14}FeI_2O_4$ $[M]^+$ 615.8331, found 615.8329.

Synthesis of Dipyridine Ligand 1. A 100 mL Schlenk flask was charged with compound **3** (270.0 mg, 0.43 mmol), 4-ethynylpyridine hydrochloride (146.8 mg, 1.05 mmol), bis(triphenylphosphine)-palladium(II) dichloride (50.6 mg, 0.04 mmol), and copper(I) iodide (8.4 mg, 0.04 mmol) under a stream of nitrogen. Freshly distilled tetrahydrofuran (10 mL) and dried triethylamine (4.0 mL) were added to the flask via syringe, and the reaction mixture was stirred overnight at 60 °C. The solvent was then evaporated, and the resulting residue was extracted with ethyl acetate over water. The organic phase was washed with brine and dried over anhydrous $MgSO_4$. Purification by silica gel column chromatography with eluent (dichloromethane/petroleum ether 3/2) yielded the orange-colored solid of compound **1** (86.1 mg, 35%). Orange crystals suitable for single-crystal X-ray analysis were grown by slow evaporation of a petroleum ether/dichloromethane/ethyl acetate solution. Mp: 204−205 °C. ^{1}H NMR ($CDCl_3$, 400 MHz): δ 3.98 (s, 3H), 5.01 (s, 5H), 4.58 (s, 2H), 5.04 (s, 2H), 7.22 (s, 4H), 8.31 (s, 2H), 8.54 (s, 4H). ^{13}C NMR($CDCl_3$, 100 MHz): δ 52.66, 68.85, 70.21, 72.47, 87.78, 92.34, 118.20, 125.47,

dx.doi.org/10.1021/jo201979d | J. Org. Chem. 2012, 77, 1148−1153

128.14, 130.23, 135.24, 149.81, 156.30, 164.87, 169.22. MS (EI): 567 (M^+, 4), 568 [$(M + 1)^+$, 1], 92 (32), 121 (33), 129 (100), 185 (74), 213 (93); HRMS (EI): exact mass calcd for $C_{33}H_{22}FeN_2O_4$ $[M]^+$ 566.0929, found 566.0931.

Self-Assembly of Hexagon 6. The dipyridyl donor ligand **1** (2.89 mg, 5.10 μmol) and the organoplatinum 120° acceptor **4** (6.84 mg, 5.10 μmol) were weighed accurately into a glass vial. To the vial was added 0.7 mL of CD_2Cl_2 solvent, and the reaction solution was then stirred at room temperature for 1 h to yield a homogeneous orange solution. The solution was then transferred into the NMR tube to collect ^1H and ^{31}P NMR spectra. Orange-colored solid product was obtained by removing the solvent under vacuum. Yield: 9.73 mg, > 99%. ^1H NMR (CD_2Cl_2, 400 MHz): δ 1.07 (t, 108H, J = 7.4 Hz), 1.28 (br, 72H), 3.98 (s, 9H), 4.30 (s, 15H), 4.70 (s, 6H), 5.11 (s, 6H), 7.50 (br, 24H), 7.63 (br, 12H), 8.43 (s, 6H), 8.64 (br, 12H). ^{31}P NMR(CD_2Cl_2, 161.9 MHz): δ 13.25 (J_{Pt-P} = 2651.9 Hz). CSI-TOF-MS, $[M - 4OTf]^{4+}$, 1281.87; $[M - 5OTf]^{5+}$, 995.65. Anal. Calcd for $C_{216}H_{270}F_{18}Fe_3N_6O_{33}P_{12}Pt_6S_6{\cdot}H_2O$: C, 45.19; H, 4.78; N, 1.46. Found: C, 44.88; H, 4.65; N, 1.35.

Self-Assembly of Hexagon 7. The donor ligand **1** (2.84 mg, 5.01 μmol) and the 180° acceptor **5** (6.18 mg, 5.00 μmol) were added to separate glass vials. To the vials containing the donor was added 0.2 mL of CH_2Cl_2, and the resulting solution was transferred to the acceptor vial charged with 0.2 mL of CH_2Cl_2. This process was repeated three times with acetone (3 × 0.15 mL) to ensure quantitative transfer of the donor to the acceptor. The reaction solution was then stirred at ambient temperature for 1 h to yield a homogeneous orange solution. Orange-colored solid product was obtained by removing the solvent under vacuum pump. Yield: 9.02 mg, > 99%. ^1H NMR (acetone-d_6, 400 MHz): δ 0.97 (t, 216H, J = 7.2 Hz), 1.29 (br, 144H), 3.86 (s, 18H), 4.21 (s, 30H), 4.59 (s, 12H), 4.97 (s, 12H), 6.99 (s, 24H), 7.68 (br, 24H), 8.28 (s, 12H), 8.89 (br, 24H). ^{31}P NMR (acetone-d_6, 161.9 MHz): δ 14.22 (J_{Pt-P} = 2716.7 Hz). CSI-TOF-MS, $[M - 4OTf]^{4+}$, 2556.03. Anal. Calcd for $C_{390}H_{516}F_{36}Fe_6N_{12}O_{60}P_{24}Pt_{12}S_{12}$: C, 43.29; H, 4.81; N, 1.55. Found: C, 43.51; H, 4.63; N, 1.35.

■ ASSOCIATED CONTENT

Supporting Information

CIF file, crystal structure, and crystallographic data of compound **1**; CSI-TOF-MS results of **6** and **7**; multinuclear NMR spectra of new compounds; cyclic voltammetry investigation. This material is available free of charge via the Internet at http://pubs.acs.org.

■ AUTHOR INFORMATION

Corresponding Author

*Email: hbyang@chem.ecnu.edu.cn.

■ ACKNOWLEDGMENTS

H.-B.Y. thanks the NSFC (Nos. 21132005 and 20902027), Shanghai Shuguang Program (No. 09SG25), Innovation Program of SMEC (No. 10ZZ32), RFDP (No. 20100076110004) of Higher Education of China, and "the Fundamental Research Funds for the Central Universities" for financial support.

■ REFERENCES

(1) (a) Lehn, J.-M. *Supramolecular Chemistry: Concepts and Perspecties*; VCH: New York, 1995. (b) Steed, J. W.; Turner, D. R.; Wallace, K. J. *Core Concepts in Supramolecular Chemistry and Nanochemistry*; John Wiley & Sons: West Sussex, U.K., 2007. (c) Steed, J. W.; Atwood, J. L. *Supramolecular Chemistry*; John Wiley & Sons: West Sussex, U.K., 2000. (d) Swiegers, G. F.; Malefetse, T. J. *Coord. Chem. Rev.* **2002**, *225*, 91.

(2) (a) Leininger, S.; Schmitz, M.; Stang, P. J. *Org. Lett.* **1999**, *1*, 1921. (b) Manna, J.; Kuehl, C. J.; Whiteford, J. A.; Stang, P. J.; Muddiman, D. C.; Hofstadler, S. A.; Smith, R. D. *J. Am. Chem. Soc.* **1997**, *119*, 11611. (c) Gianneschi, N. C.; Masar, M. S.; Mirkin, C. A. *Acc. Chem. Res.* **2005**, *38*, 825. (d) Cotton, F. A.; Lin, C.; Murillo, C. A. *Acc. Chem. Res.* **2001**, *34*, 759. (e) Fiedler, D.; Leung, D. H.; Bergman, R. G.; Raymond, K. N. *Acc. Chem. Res.* **2005**, *38*, 351. (f) Liu, S.; Han, Y.-F.; Jin, G.-X. *Chem. Soc. Rev.* **2007**, *36*, 1543. (g) Han, Y.; Jia, W.; Yu, W.; Jin, G. *Chem. Soc. Rev.* **2009**, *38*, 3419. (h) Chakrabarty, R.; Mukherjee, P. S.; Stang, P. J. *Chem. Rev.* **2011**, *111*, 6810.

(3) (a) Wang, P.; Moorefield, C. N.; Newkome, G. R. *Angew. Chem., Int. Ed.* **2005**, *44*, 1679. (b) Wang, J.; Li, X.; Lu, X.; Chan, Y.; Moorefield, C. N.; Wesdemiotis, C.; Newkome, G. R. *Chem.—Eur. J.* **2011**, *17*, 4830. (c) You, C.; Würthner, F. *J. Am. Chem. Soc.* **2003**, *125*, 9716. (d) Sun, W.-Y.; Kusukawa, T.; Fujita, M. *J. A. Chem. Soc.* **2002**, *124*, 11570. (e) Ulmann, P. A.; Braunschweig, A. B.; Lee, O.-S.; Wiester, M. J.; Schatz, G. C.; Mirkin, C. A. *Chem. Commun.* **2009**, 5121. (f) Han, Y.-F.; Jia, W.-G.; Lin, Y.-J.; Jin, G.-X. *Organometallics* **2008**, *27*, 5002. (g) Han, Y.-F.; Li, H.; Jin, G.-X. *Chem. Commun.* **2010**, *46*, 6879.

(4) (a) Yang, H.-B.; Das, N.; Huang, F.; Hawkridge, A. M.; Muddiman, D. C.; Stang, P. J. *J. Am. Chem. Soc.* **2006**, *128*, 10014. (b) Yang, H.-B.; Hawkridge, A. M.; Huang, S. D.; Das, N.; Bunge, S. D.; Muddiman, D. C.; Stang, P. J. *J. Am. Chem. Soc.* **2007**, *129*, 2120. (c) Zhao, G.-Z.; Chen, L.-J.; Wang, C.-H.; Yang, H.-B.; Ghosh, K.; Zheng, Y.-Y.; Lyndon, M. M.; Muddiman, D. C.; Stang, P. J. *Organometallics* **2010**, *29*, 6137.

(5) (a) Chi, K.-W.; Addicott, C.; Stang, P. J. *J. Org. Chem.* **2004**, *69*, 2910. (b) Huang, F.; Yang, H.-B.; Das, N.; Maran, U.; Arif, A. M.; Gibson, H. W.; Stang, P. J. *J. Org. Chem.* **2006**, *71*, 6623. (c) Yang, H.-B.; Ghosh, K.; Northrop, B. H.; Zheng, Y.-R.; Lyndon, M. M.; Muddiman, D. C.; Stang, P. J. *J. Am. Chem. Soc.* **2007**, *129*, 14187. (d) Ghosh, K.; Yang, H.-B.; Northrop, B. H.; Lyndon, M. M.; Zheng, Y.-R.; Muddiman, D. C.; Stang, P. J. *J. Am. Chem. Soc.* **2008**, *130*, 5320. (e) Zhu, K.; He, J.; Li, S.; Liu, M.; Wang, F.; Zhang, M.; Abliz, Z.; Yang, H.-B.; Li, N.; Huang, F. *J. Org. Chem.* **2009**, *74*, 3905. (f) Xu, X.-D.; Yang, H.-B.; Zheng, Y.-R.; Ghosh, K.; Lyndon, M. M.; Muddiman, D. C.; Stang, P. J. *J. Org. Chem.* **2010**, *75*, 7373.

(6) (a) Yang, H.-B.; Ghosh, K.; Zhao, Y.; Northrop, B. H.; Lyndon, M. M.; Muddiman, D. C.; White, H. S.; Stang, P. J. *J. Am. Chem. Soc.* **2008**, *130*, 839. (b) Ghosh, K.; Zhao, Y.; Yang, H.-B.; Northrop, B. H.; White, H. S.; Stang, P. J. *J. Org. Chem.* **2008**, *73*, 8553. (c) Ghosh, K.; Hu, J.; Yang, H.-B.; Northrop, B. H.; White, H. S.; Stang, P. J. *J. Org. Chem.* **2009**, *74*, 4828. (d) Zhao, G.-Z.; Li, Q.-J.; Chen, L.-J.; Tan, H.; Wang, C.-H.; Lehman, D. A.; Muddiman, D. C.; Yang, H.-B. *Organometallics* **2011**, *30*, 3637.

(7) Northrop, B. H.; Yang, H.-B.; Stang, P. J. *Chem. Commun.* **2008**, 5896.

(8) (a) Stang, P. J.; Cao, D. H.; Chen, K.; Gray, G. M.; Muddiman, D. C.; Smith, R. D. *J. Am. Chem. Soc.* **1997**, *119*, 5163. (b) Addicott, C.; Oesterling, I.; Yamamoto, T.; Mullen, K.; Stang, P. J. *J. Org. Chem.* **2005**, *70*, 797. (c) Das, N.; Stang, P. J.; Arif, A. M.; Campana, C. F. *J. Org. Chem.* **2005**, *70*, 10440. (d) Jude, H.; Sinclair, D. J.; Das, N.; Sherburn, M. S.; Stang, P. J. *J. Org. Chem.* **2006**, *71*, 4155. (e) Deng, H.; Doonan, C. J.; Furukawa.; Ferreira, H.; R. B.; Towne, J.; Knobler, C. B.; Wang, B.; Yaghi, O. M. *Science* **2010**, *327*, 846.

(9) (a) Tominaga, M.; Suzuki, K.; Murase, T.; Fujita, M. *J. Am. Chem. Soc.* **2005**, *127*, 11950. (b) Murase, T.; Sato, S.; Fujita, M. *Angew. Chem., Int. Ed.* **2007**, *46*, 5133. (c) Sato, S.; Iida, J.; Suzuki, K.; Kawano, M.; Ozeki, T.; Fujita, M. *Science* **2006**, *313*, 1273. (d) Murase, T.; Sato, S.; Fujita, M. *Angew. Chem., Int. Ed.* **2007**, *46*, 1083. (e) Sun, W.; Kusukawa, T.; Fujita, M. *J. A. Chem. Soc.* **2002**, *124*, 11570. (f) Suzuki, K.; Kawano, M.; Sato, S.; Fujita, M. *J. Am. Chem. Soc.* **2007**, *129*, 10652.

(10) Zhao, L.; Ghosh, K.; Zheng, Y.-R.; Stang, P. J. *J. Org. Chem.* **2009**, *74*, 8516.

(11) (a) Collinson, M. M. *Acc. Chem. Res.* **2007**, *40*, 777. (b) van Staveren, D. R.; Metzler-Nolte, N. *Chem. Rev.* **2004**, *104*, 5931. (c) Astruc, D. *Acc. Chem. Res.* **2000**, *33*, 287. (d) Belin, C.; Astruc, D. *Angew. Chem., Int. Ed.* **2006**, *45*, 132. (e) Ornelas, C.; Mery, D.; Blais,

J.-C.; Cloutet, E.; Aranzaes, J. R.; Astruc, D. *Angew. Chem., Int. Ed.* **2005**, *44*, 7399.
(12) Matsuda, H.; Ayabe, Y. Z. *Electrochem* **1955**, *59*, 494.